

## CO<sub>2</sub> FLUX SURVEYS FOR GEOTHERMAL EXPLORATION IN ARID ENVIRONMENTS

Mark Harvey<sup>1</sup>, Guillermo Chavez<sup>2</sup> and Marcos Delgado

<sup>1</sup>Harvey Geoscience Ltd, 51 Gifford Rd, West Hartford, Connecticut, 06119, USA

<sup>2</sup>Polaris Energy Nicaragua, San Jacinto Tizate, León, Nicaragua

e-mail: mark@harveygeoscience.com

### **ABSTRACT**

A 20 km<sup>2</sup> soil CO<sub>2</sub> flux survey was undertaken in and around the San Jacinto-Tizate geothermal power project, Nicaragua. Conditions during the survey were undertaken in the dry season (March-April 2017), and were dry and hot for the entire survey period. This provided a high-quality CO<sub>2</sub> flux dataset with apparently negligible interference from biological gas flux. The survey showed a broad area of low CO<sub>2</sub> flux (LFZ), which surrounds the central production area. This may result from a low permeability capping formation; the capping formation blocks CO<sub>2</sub> flux from reaching the surface. The LFZ partly encircles a high-flux zone (HFZ), an area of relatively high CO<sub>2</sub> flux that occurs to the NNW of the steamfield. The HFZ is closely associated with i) a magnetic high anomaly, previously interpreted to result from unaltered material, ii) MT resistivity high, and iii) watershed catchment boundaries. Together, these observations suggest the area is hydrologically isolated from the central production area, and may lack a reservoir. Results suggest CO<sub>2</sub> gas flux surveys are particularly well suited to arid environments (e.g. Basin and Range, Atacama Desert), or in areas with a pronounced dry season (Central America, East Africa). Under these conditions, signal interference from biological soil CO<sub>2</sub> flux is greatly reduced, and CO<sub>2</sub> flux surveys may be able to identify the clay cap as a zone of relatively low CO<sub>2</sub> flux. This is a key objective of well targeting and geothermal exploration.

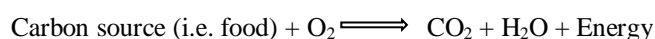
### **INTRODUCTION**

San Jacinto is a high temperature geothermal system located on Los Marrabios volcanic chain, Nicaragua. The first exploration wells were drilled at San Jacinto in the early 1990's. A demonstration plant was commissioned in 2005 (10 MW), then expanded to the current installed capacity (77 MW). Surface thermal features (springs, steaming ground and small fumaroles) occur at low elevation near the main production area at El Tizate, and near the San Jacinto village (*Figure 1*).

Soil gas flux measurements allow the identification of subsurface geothermal activity that may not otherwise be evident. As CO<sub>2</sub> is the major component of typical geothermal gases, and is readily detectable, it is the most appropriate component to focus on.

Soil diffuse CO<sub>2</sub> flux is the measurement of CO<sub>2</sub> emission from the ground to the atmosphere. Broadly speaking, CO<sub>2</sub> flux may have one of two sources: deep or shallow (geothermal or biogenic, respectively). Much deeply sourced CO<sub>2</sub> may originate from a degassing magma, emplaced at some depth beneath the surface (Chiodini *et al.*, 1996). Biological soil CO<sub>2</sub> flux originates from metabolic processes occurring in the shallow soil layer (i.e. surface soils overlying geological formations). The dominant respiration sources are soil roots, microbes, and micro-fauna (small animals) (Raich and Schlesinger, 1992).

The concept of microbial soil CO<sub>2</sub> flux may be somewhat unfamiliar to the geothermal scientist or geologist. However, the principal is intuitive; the process of microbial respiration in the soil is like animal respiration, per the generalized oxidation reaction:



The degree of interference (i.e. to the geothermal CO<sub>2</sub> flux signal) caused by this reaction may be strongly affected by the degree of biological activity in the soil at the time of measurement. This in turn is expected to be affected by soil moisture, with very dry (dehydrated) soils having low to negligible CO<sub>2</sub> flux.

A 609-point soil CO<sub>2</sub> gas flux survey was undertaken at San Jacinto during the wet season (July) 2011, to determine if mapped faults were associated with elevated CO<sub>2</sub> flux in an area of 20 km<sup>2</sup> around El Tizate (Harvey *et al.*, 2011; **Figure 1**). This survey found relatively high mean CO<sub>2</sub> flux (51 g m<sup>-2</sup> d<sup>-1</sup>) that indicated possible biological signal interference.

This paper provides results from a repeat survey conducted in the dry season (March-April) 2017.

## **SURVEY METHODS AND DESIGN**

Soil CO<sub>2</sub> flux measurements were made according to an approximately 100m x 400m grid survey design (**Figure 1**). Some measurements were made at closer spacing (~20m) across previously mapped faults to provide higher resolution in these areas.

Soil CO<sub>2</sub> flux measurements were made using a West Systems portable soil gas flux meter (accumulation chamber method). The accumulation method calculates CO<sub>2</sub> flux by placing a 200-mm diameter accumulation chamber on the soil surface and pressing it into the soil to obtain a seal. Gases flowing into the chamber are pumped to an infrared gas analyser and the increase in CO<sub>2</sub> concentration inside the chamber over time is recorded by the instrument. The rate of concentration increase is proportional to flux.

The CO<sub>2</sub> flux data set was interpolated by the Sequential Gaussian Simulation (sGs) algorithm within SGeMS software (Remy *et al.*, 2009). sGs is a stochastic method that provides more realistic flux maps than kriging (kriging reproduces neither the histogram nor variogram statistics of the original dataset). In addition, sGs provides smaller standard deviation than other methods when deriving total flow for a survey area (Cardellini *et al.*, 2003), an important advantage for monitoring applications. CO<sub>2</sub> flux was also interpolated by Kriging for comparison with 2011 results. A single grid was generated by interpolation algorithms (20x20m).

Raw data was subject to the following analysis steps: (1) computation of the experimental variogram; (2) modelling the variogram for each data set; and (3) sGs. Datum for all maps is WGS84.

Watershed basins (catchments) for the survey area were delineated using SAGA (System for Automated Geoscientific Analyses), GIS software developed for processing digital elevation models (DEM) (Olaya and Conrad, 2009); the *Fill Sinks* tool was applied to a 20m and 5m DEM.

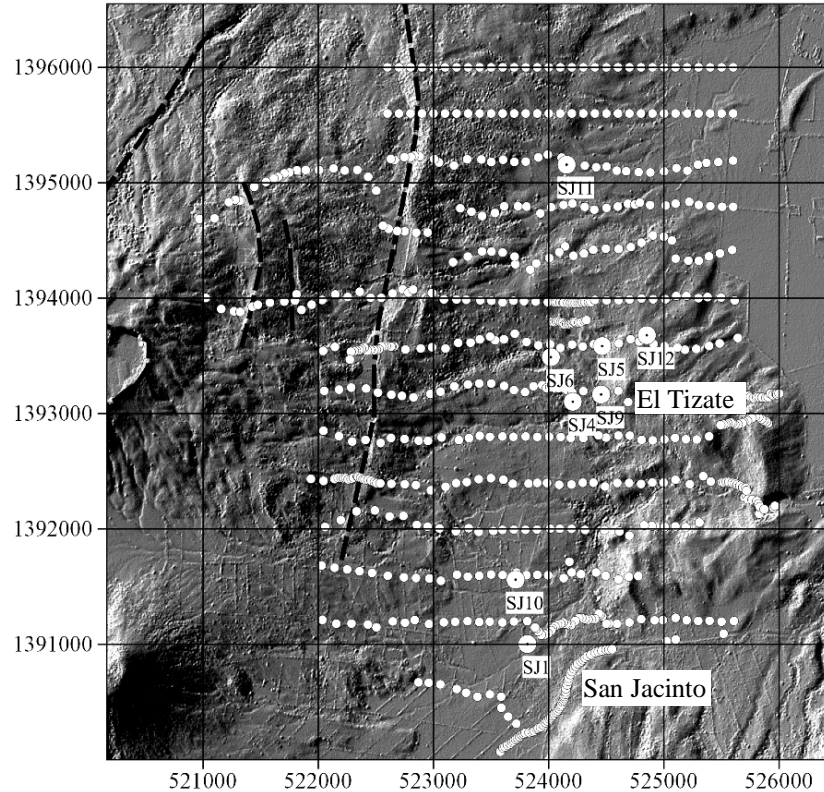


**Figure 1: CO<sub>2</sub> flux survey measurement locations (white points) at El Tizate steam field and San Jacinto. Black dash lines show previously interpreted faults. Geothermal wells are labelled.**

### **DETERMINATION OF THE BIOLOGICAL BACKGROUND**

In order to evaluate whether the soil CO<sub>2</sub> flux measurements were due to background (biological) soil conditions or geothermal sources, a cumulative probability plot was generated (**Figure 4**). Reimann *et al.* (2005) note that inflection or break points in cumulative probability plots can be used to distinguish the presence of multiple populations. However, no such break points are apparent in the plot, consistent with a single population.

Conditions during the 2017 survey were consistently dry and hot (average ambient air temperature 36°C), with practically no rain for the entire survey period (February 28 – April 6). The average of the 2017 CO<sub>2</sub> flux dataset (6 g m<sup>-2</sup> d<sup>-1</sup>) is much lower than the average value for the 2011 survey (51 g m<sup>-2</sup> d<sup>-1</sup>)(**Figure 2 - Figure 3**). It is probable the hot, dry conditions dehydrated the soil and eliminated most biological activity.

To confirm this, the effect of soil moisture was tested by comparing CO<sub>2</sub> flux from dry and moist soils nearby a sprinkler at San Jacinto. Soil near the sprinkler was moist and covered with live grass. Adjacent soil (~20m distance) was dry and without vegetation, typical of survey conditions (**Figure 5B**). Six measurements were made on each area and show the moist soils had CO<sub>2</sub> flux 5-6 times higher than nearby dry soils (**Figure 5B**). The dry soil average (7.5 g m<sup>-2</sup> d<sup>-1</sup>) is close to the 2017 dataset average (5.7 g m<sup>-2</sup> d<sup>-1</sup>), whereas the moist soil average (53 g m<sup>-2</sup> d<sup>-1</sup>) is close to the 2011 average (51 g m<sup>-2</sup> d<sup>-1</sup>). This result confirms the dry conditions have greatly reduced biological activity in the soil. It is assumed biological CO<sub>2</sub> flux in the 2017 dataset is negligible.

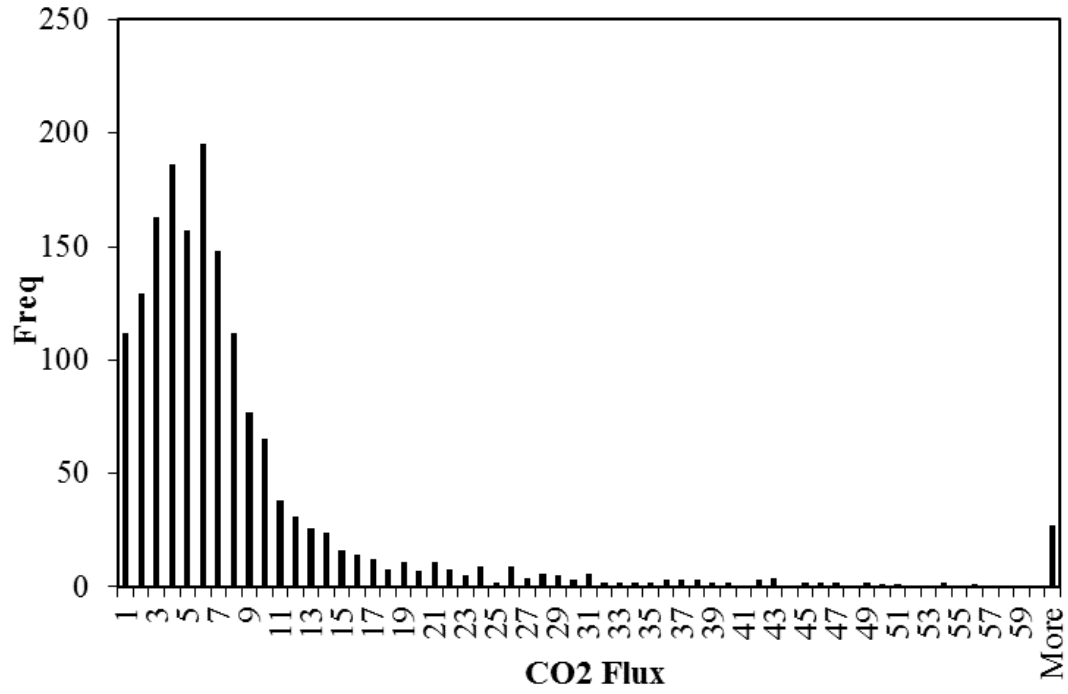


Figure 2: Histogram of 2017 CO<sub>2</sub> flux results (units are g m<sup>-2</sup> d<sup>-1</sup>).

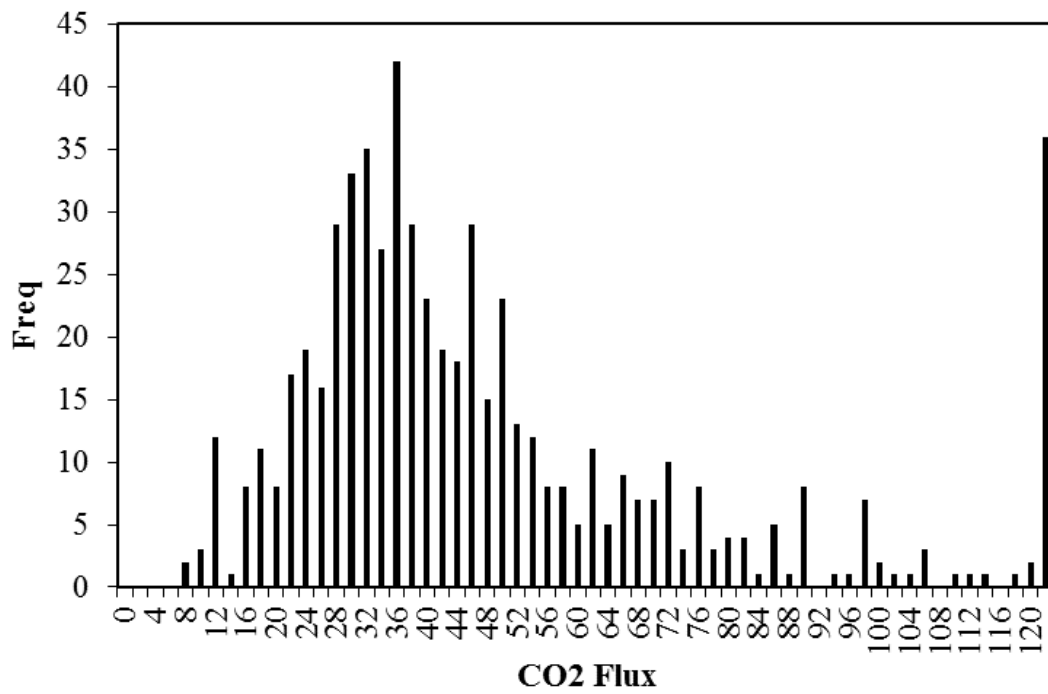


Figure 3: Histogram of 2011 CO<sub>2</sub> flux results (units are g m<sup>-2</sup> d<sup>-1</sup>).

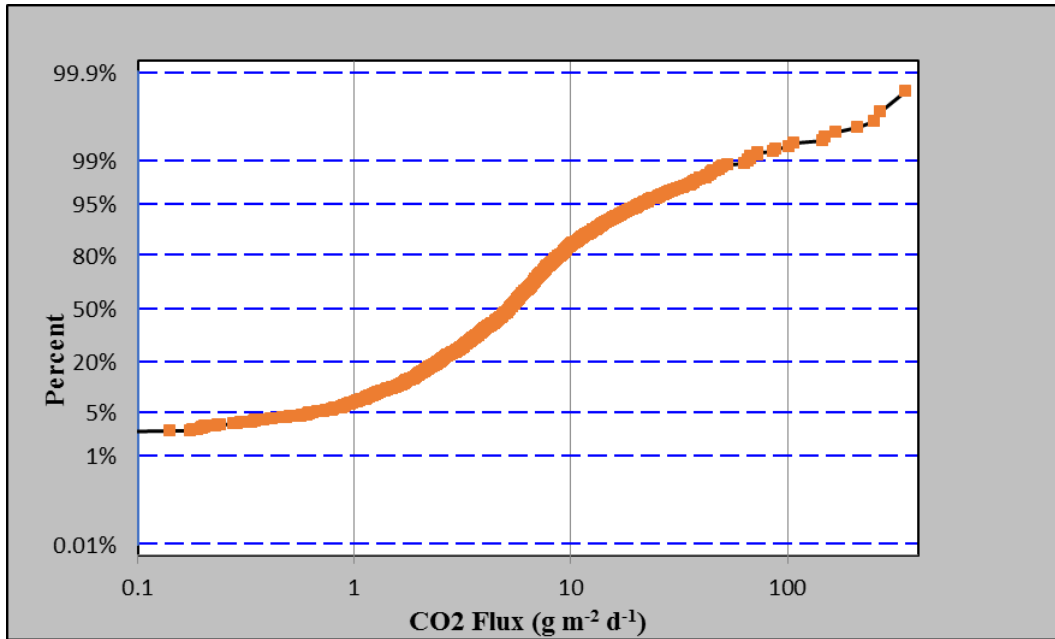


Figure 4: Cumulative probability plot (all data). Note: the curve is smooth with no obvious breaks.

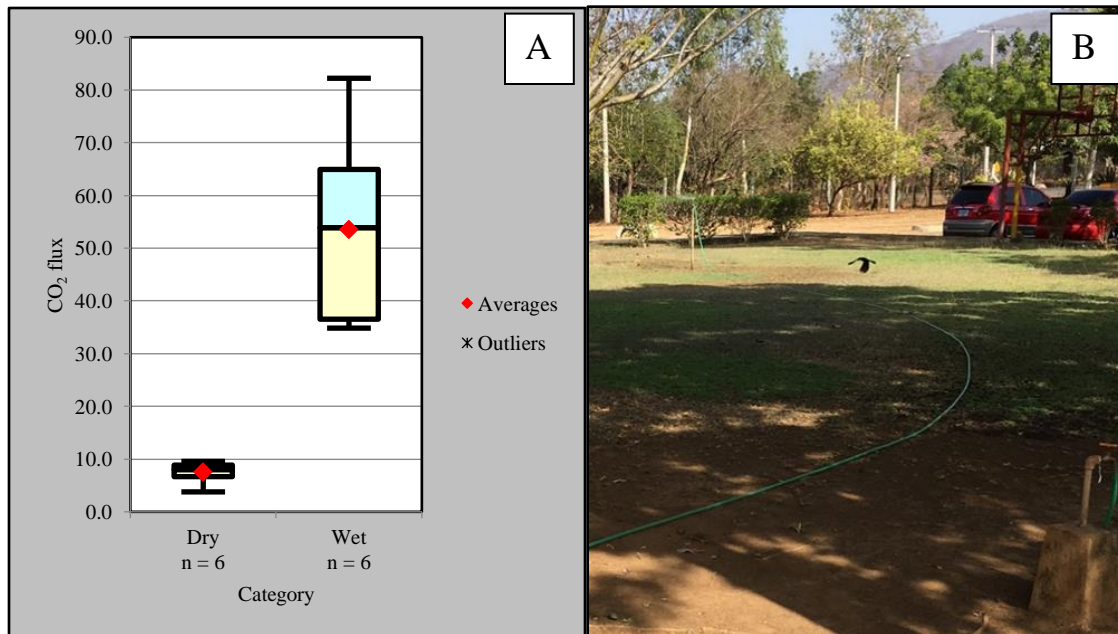


Figure 5: (A) Box and whisker plot showing results of experiment comparing CO<sub>2</sub> flux from adjacent soils: moist versus dry. Note i) dry soil average (7.5 g m<sup>-2</sup> d<sup>-1</sup>) is close to the 2017 dataset average (5.7 g m<sup>-2</sup> d<sup>-1</sup>), and ii) watered soil average (53 g m<sup>-2</sup> d<sup>-1</sup>) is close to the 2011 average (51 g m<sup>-2</sup> d<sup>-1</sup>). (B) photo of experiment area at offices near San Jacinto village. Note: dry dirt in foreground lacks vegetation. Hose leads to the sprinkler and grass area.

## SOIL CO<sub>2</sub> FLUX SURVEY RESULTS

609 measurements were collected over 14 field days, between 28 February and 13 March 2017. Soil CO<sub>2</sub> flux results are shown as a pixel plot (*Figure 6*).

Key observations from *Figure 6*:

- A. El Tizate production area falls within a low flux zone (LFZ), an area of low CO<sub>2</sub> flux that broadens to the north and narrows to the south (*Figure 6A*). The zone is larger, but of a similar shape to the boundary of the narrow swarm of N-S/NNW-SSE extensional structures, that spreads and shallows northwards (*Figure 6C*), identified by Norini (2016).
- B. The LFZ is bounded to the NNW by a 1.7km<sup>2</sup> area of relatively high CO<sub>2</sub> flux (*Figure 6B*). This high flux zone (HFZ) is bounded to the west by the Los Tablonas fault.

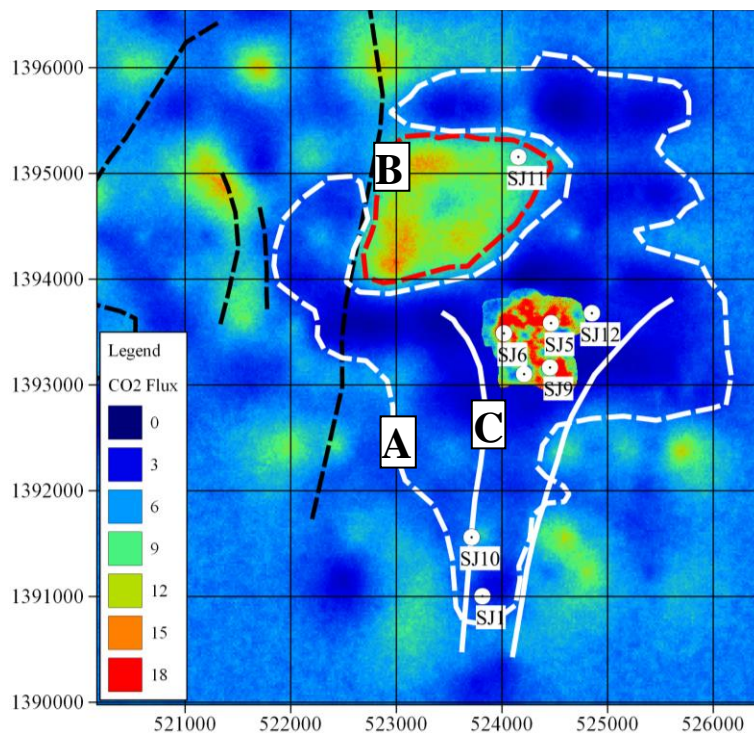


**Figure 6:** CO<sub>2</sub> flux results interpolated by sGs. Note: (A) white dash shows LFZ boundary, (B) HFZ area inside red dash, and (C) structural swarm (Norini, 2016)(solid white). Black dash lines are faults. Geothermal wells are labelled. CO<sub>2</sub> flux units are g m<sup>-2</sup> d<sup>-1</sup>. Note: Large area of anomalous CO<sub>2</sub> flux in central production area is associated with thermal ground and based on results from a separate, high-density survey in that area.



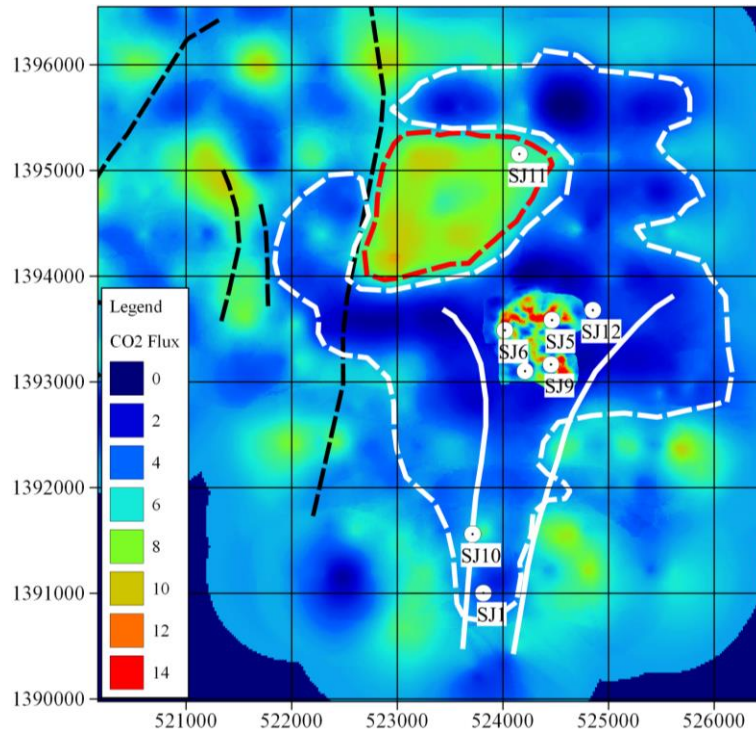


**Figure 7: CO<sub>2</sub> flux results interpolated by Simple Kriging. Note Simple Kriging produces a similar result to sGs result (Figure 6). Black dash lines are faults. Geothermal wells are labelled. CO<sub>2</sub> flux units are g m<sup>-2</sup> d<sup>-1</sup>.**

## DISCUSSION

### Soil Conditions

Conditions during the 2017 survey were dry and hot (average ambient air temperature ~36°C) for the entire survey period (February 28 – April 6). The average CO<sub>2</sub> flux (6 g m<sup>-2</sup> d<sup>-1</sup>) is much lower than the average value for the 2011 survey (51 g m<sup>-2</sup> d<sup>-1</sup>)(Figure 2 - Figure 3). Equipment and measurement locations (±5m) were the same for both surveys. The difference in the averages results from shallow soil conditions; the previous 2011 survey occurred in July when regular rainfall meant that the soil was biologically active.

This interpretation is supported by an experiment conducted at San Jacinto, where CO<sub>2</sub> flux measurements compared watered to non-watered soils, and showed dry conditions greatly reduce biological activity in the soil. It follows the 2011 CO<sub>2</sub> flux results must now be regarded as severely compromised by biological interference; the degree of biological interference, now obvious, was not known in 2011. The 2017 survey has provided a high-quality data set and the following discussion assumes negligible interference from biological gas flux.

### CO<sub>2</sub> flux, structure and watershed basins

The El Tizate thermal area and central production zone falls within broad low flux zone (LFZ)(7.5 km<sup>2</sup>, average ~4 g m<sup>-2</sup> d<sup>-1</sup>) that broadens to the north and tapers to the south (**Figure 6A**). The LFZ is similar in shape to the narrow swarm of N-S/NNW-SSE extensional structures, that spreads and shallows northwards (**Figure 6C**)(Norini, 2016). Relatively small areas of steam heated ground and associated intense CO<sub>2</sub> flux degassing that penetrate a much larger clay cap have been noted elsewhere (Werner *et al.*, 2004; Rissmann *et al.*, 2012, Hanson *et al.*, 2014).

It is possible the LFZ at El Tizate is associated with the structural swarm, and results from two factors, i) rising CO<sub>2</sub> is blocked from reaching the surface by impermeable hydrothermal clays (the clay cap), and/or ii) and/or focussing of reservoir degassing through the El Tizate thermal areas and production wells. The LFZ is bounded to the NNW by the HFZ, a 1.7km<sup>2</sup> zone of relatively high CO<sub>2</sub> flux (average ~10 g m<sup>-2</sup> d<sup>-1</sup>). The area is closely associated with a magnetic

high anomaly, previously interpreted to result from unaltered material (i.e. unaffected by hydrothermal activity)(**Figure 8**)(SKM, 2011).

A previous MT survey showed the base of the MT conductor deepens in this area (Figure 9)(SKM, 2011). Preliminary results from a more recent MT survey (2017) suggest a shallow clay cap is absent in this area (Figure 10)(G. Chavez, Pers. Comms). There is no gravity anomaly associated with the HFZ area (SKM, 2011).

Output from the watershed modelling shows the southern and western boundaries of the HFZ/magnetic anomaly are closely matched with catchment boundaries (Figure 11). In comparison, the El Tizate thermal area and steamfield lies within the adjacent southern watershed, which has an extensive catchment to the west (higher elevation areas to the west). Modelling was repeating using a 5m spatial resolution DSM, and gave a similar result (Figure 12).

### **Implications for the conceptual model of San Jacinto hydrothermal reservoir**

The San Jacinto reservoir results from three critical inputs that converge at El Tizate:

- Heat: intrusive
- Permeability: structural swarm
- Recharge: large western catchment

It is certain that meteoric recharge (rain) infiltrates soils at higher elevation in the west then drains eastwards. El Tizate is located within a topographic low where subsurface recharge forms a reservoir; hills immediately to the east of the production area form the eastern catchment boundary, slowing or preventing the subsurface flow from draining to the low lands further east (Figure 13). The captive recharge is heated, and acidified by CO<sub>2</sub> and H<sub>2</sub>S rising from beneath. Once acidified, the fluid alters volcanics to clay. An analogous situation exists in the Taupo Volcanic Zone (New Zealand), where hydrothermal systems are also supplied by meteoric recharge (Giggenbach, 1995). Most systems are located along the Waikato River (9 out of 13), which is the primary hydrological drainage channel and topographic low for the Taupo graben (Harvey *et al.*, 2015a; Ratouis and Zarrouk, 2015). The importance of surface topography to system recharge (and the effects on measured CO<sub>2</sub> flux), is discussed by Harvey *et al.* (2015a).

In contrast to El Tizate, the HFZ lies within the adjacent watershed to the north, and lacks i) a large western catchment, and ii) confining hills to the east. Simply put, there may be no water to engage in water-rock interaction; this would explain the co-occurrence of CO<sub>2</sub> flux, magnetic high and shallow resistivity high in the HFZ area. This observation led to the conclusion that El Tizate and the HFZ are hydrologically isolated, and the prediction that fluids re-injected into the HFZ would not support pressure in the El Tizate production reservoir (Harvey Geoscience, 2017).

This prediction was recently validated by the new re-injection well SJ11-2 (completed June 2017), which penetrates to the HFZ and encountered massive permeability (1100 tons per hour at the bottom of the hole)(**Figure 11**). The well has limited connected to the main production reservoir based on the lack of pressure support to the nearby production reservoir.

### **Total CO<sub>2</sub> emissions**

The 2017 CO<sub>2</sub> flux average (6 g m<sup>-2</sup> d<sup>-1</sup>) multiplied by the survey area (~20km<sup>2</sup>) gives an estimate of natural soil diffuse CO<sub>2</sub> emissions during the survey period: 6 g m<sup>-2</sup> d<sup>-1</sup> x 2.0 x 10<sup>7</sup> m<sup>2</sup> = 120 tons CO<sub>2</sub> per day. This is almost twice CO<sub>2</sub> emissions from the power plant: 25,000 tons per year = 69 tons per day (G. Chavez, Pers Comms.)

### **Comparison with the 2011 survey**

It is difficult to compare the 2011 and 2017 surveys; in 2011, a threshold between biological/geothermal CO<sub>2</sub> flux populations was assumed (13 g m<sup>-2</sup> d<sup>-1</sup>), and “geothermal anomalies” above this threshold were discussed. In 2017, the dataset is assumed to be a single population of geothermal flux (i.e. with negligible biological CO<sub>2</sub> flux).

Interpolated CO<sub>2</sub> flux from the 2017 survey (Figure 7) bears little resemblance to the 2011 map (**Figure 14**). The simplest explanation for the discrepancy is the dryer survey conditions in 2017; many “anomalies” reported in 2011 were apparently of biological origin.



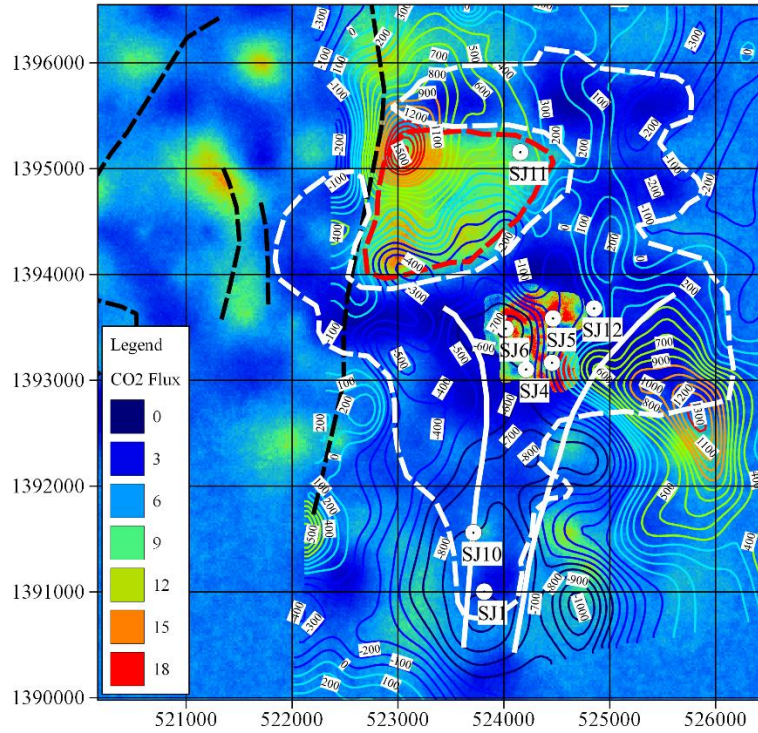


**Figure 8.** CO<sub>2</sub> Flux results (sGs) plus mag survey contours (nT, reduction to pole). Note: i) HFZ to NNW of steamfield (inside red dash) corresponds to mag high, and ii) LFZ (white dash) corresponds to structural swarm and demagnetized area (SKM, 2011). Black dash lines show Los Tablones and La Joya faults.

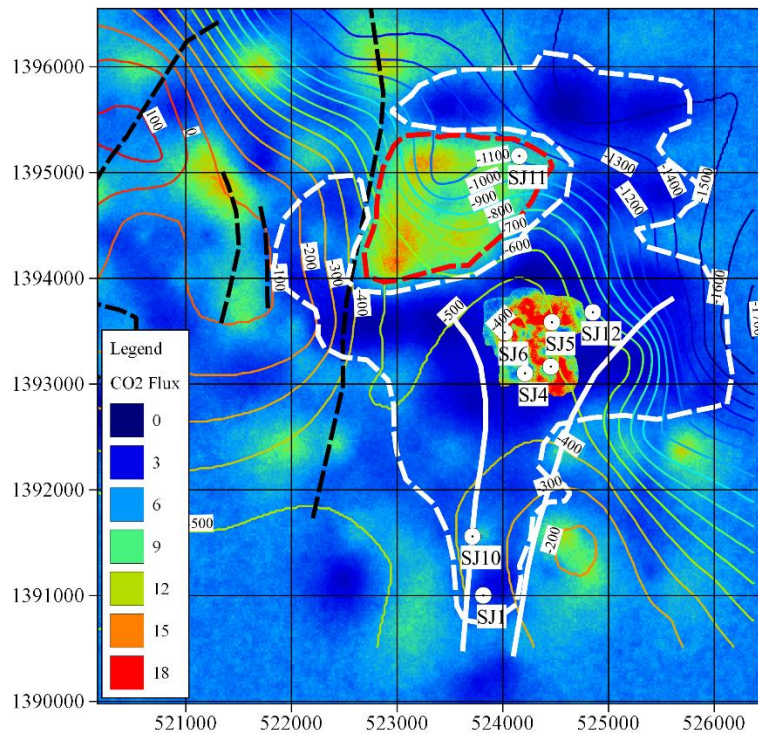


**Figure 9.** CO<sub>2</sub> flux results (sGs) plus MT survey contours (depth to base of conductor)(SKM, 2011). Note: i) HFZ to NNW of steamfield (inside red dash boundary) corresponds to deepening of base of conductor, and ii) LFZ (white dash line) corresponds to structural swarm and MT shallowing of base of conductor. Black dash lines show Los Tablones and La Joya faults.

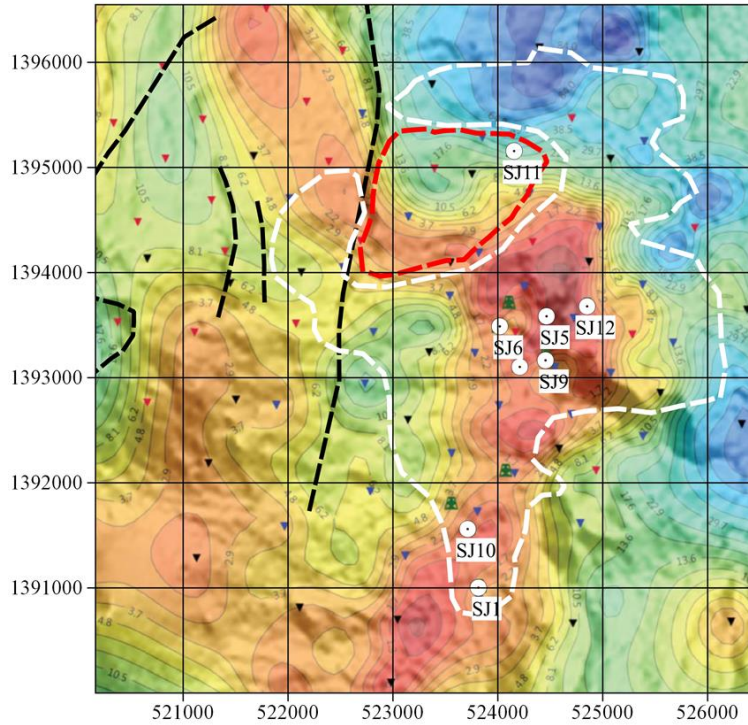


**Figure 10. Preliminary results from 2017 MT survey: 3D MT inversion – Resistivity at 0m mrsi (ohm.m). Note: HFZ (red dash) corresponds to approx. position of resistivity high at shallow depth. Black dash show Los Tablones and La Joya faults. White dash shows LFZ.**

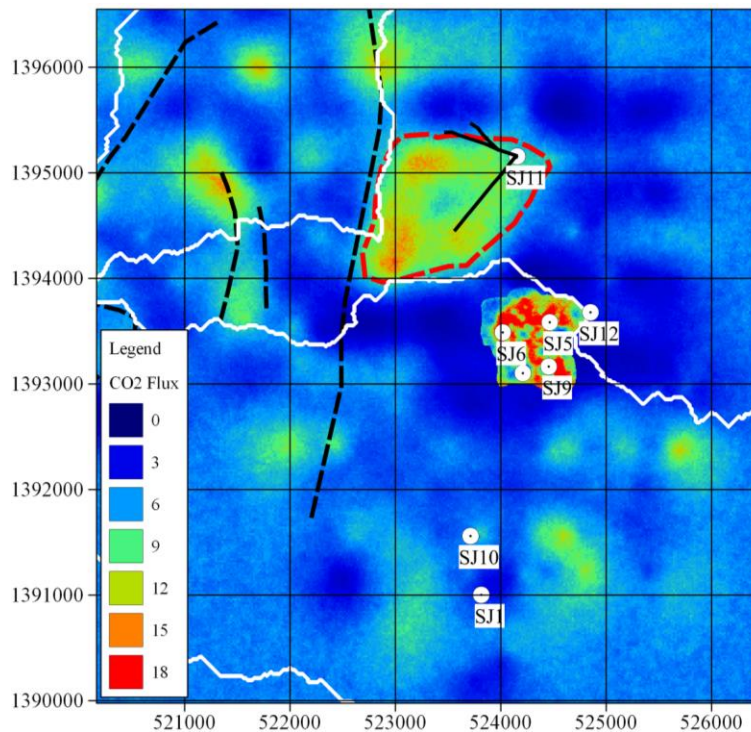


**Figure 11. Watershed boundaries (solid white lines, derived from 20m DSM) overlaid on CO<sub>2</sub> flux results (sGs). Note: HFZ (red dash boundary) is bounded to the south and west by watershed boundaries (western watershed boundary is the Los Tablones fault). Black dash show Los Tablones and La Joya faults. Solid black lines show well tracks follow the northern margin of HFZ (SJ11-1), and penetrate HFZ (SJ11-2).**



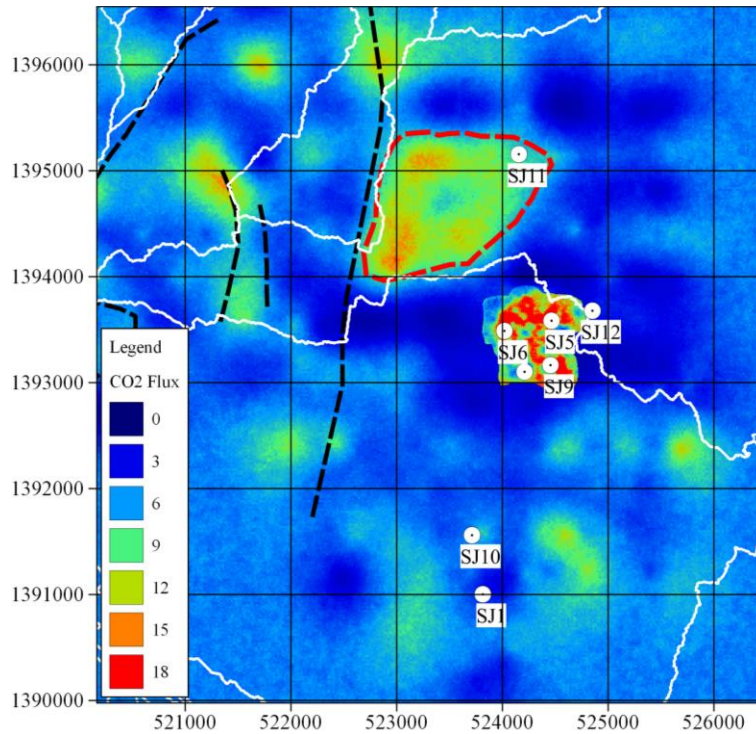


**Figure 12. Watershed boundaries (solid white lines, derived from 5m DSM) overlaid on CO<sub>2</sub> flux results (sGs). Note: HFZ (inside red dash boundary) is bounded to south & west by watershed boundaries (western watershed boundary is the Los Tablones fault). Black dash lines show Los Tablones and La Joya faults.**



**Figure 13. View of El Tizate production area looking eastwards and down slope into the El Tizate production area valley from the rim of the Los Tablones fault. Recharge flows down toward El Tizate from Los Tablones and the higher elevation catchment to the west. Recharge forms a reservoir at the El Tizate topographic low; note the hill immediately to the east of the production area prevents recharge escaping further east. Recharge is heated and acidified (by CO<sub>2</sub>, H<sub>2</sub>S), and alters volcanics to clay. White boundary is the LFZ that results from the clay cap. Red boundary encloses HFZ to the north, located on adjacent catchment. Image with vertical exaggeration from Google Earth.**

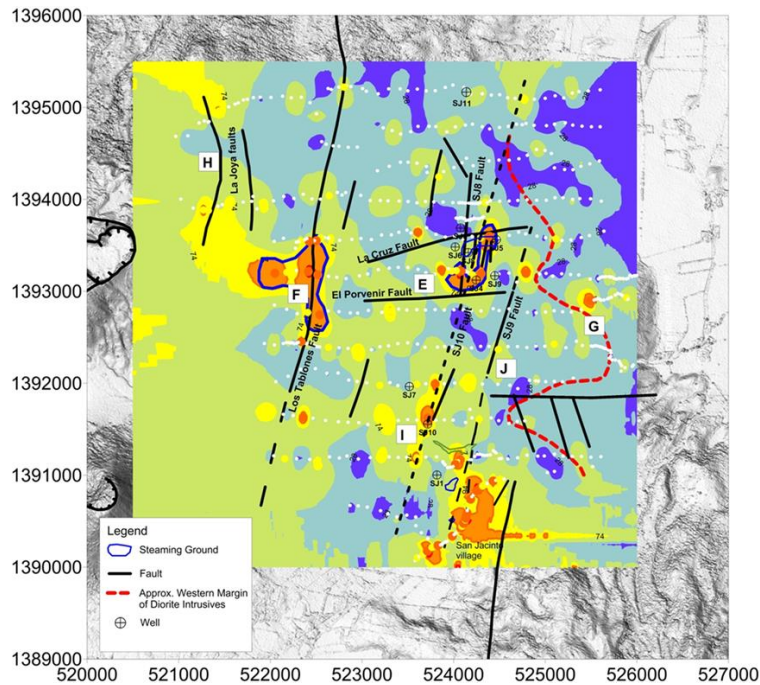


**Figure 14. CO<sub>2</sub> flux survey results from 2011, interpolated by Simple Kriging (Harvey et al., 2011).**

## **CONCLUSIONS**

Conditions during the 2017 survey were dry and hot for the entire survey period. This has provided a high-quality CO<sub>2</sub> flux dataset with apparently negligible interference from biological gas flux.

A broad area of low CO<sub>2</sub> flux (LFZ) surrounds the central production area. This may result from a low permeability capping formation and/or depletion of reservoir CO<sub>2</sub> because of production. The area partly encircles an area of relatively high CO<sub>2</sub> flux (HFZ) that occurs to the NNW of the steamfield. The HFZ is closely associated with i) a magnetic high anomaly, previously interpreted to result from unaltered material, ii) MT resistivity high, and iii) watershed catchment boundaries. Together with recent drilling results, these observations show the HFZ area is hydrologically isolated from the central production area.

Results suggest CO<sub>2</sub> gas flux surveys are particularly well suited to arid environments (e.g. Basin and Range, Atacama Desert), or in areas with a pronounced dry season (Central America, East Africa). Under these conditions, CO<sub>2</sub> flux surveys may be able to identify the clay cap as a zone of relatively low CO<sub>2</sub> flux, a key objective of well targeting and geothermal exploration. In wet climates, or where biological activity is suspected in the soil, it is recommended that future surveys combine CO<sub>2</sub> flux measurements with <sup>13</sup>C<sub>2</sub> isotope analysis to identify biological signal interference (Harvey *et al.*, 2015b).

## **ACKNOWLEDGMENTS**

We would like to acknowledge and thank PENZA for providing support to this project, and for allowing publication of results.

## REFERENCES

- Cardellini, C., G. Chiodini, and F. Frondini (2003), Application of stochastic simulation to CO<sub>2</sub> flux from soil: Mapping and quantification of gas release, *J. Geophys. Res.: Solid Earth (1978–2012)*, 108.
- Chiodini, G., F. Frondini, and B. Raco (1996), Diffuse emission of CO<sub>2</sub> from the Fossa crater, Vulcano Island (Italy) *Bull. Volcan.*, 58, 41-50.
- Fridriksson, T., B. R. Kristjánsson, H. Ármannsson, E. Margrétardóttir, S. Ólafsdóttir, and G. Chiodini (2006), CO<sub>2</sub> emissions and heat flow through soil, fumaroles, and steam heated mud pools at the Reykjanes geothermal area, SW Iceland, *Appl. Geochem.*, 21, 1551-1569.
- Giggenbach, W. F. (1995), Variations in the chemical and isotopic composition of fluids discharged from the Taupo Volcanic Zone, New Zealand, *J. Volcanol. Geotherm. Res.*, 68, 89-116.
- Hanson, M.C., Oze, C., and Horton, T.W. (2014), Identifying blind geothermal systems with soil CO<sub>2</sub> surveys. *Applied Geochemistry*, 50, 106–114.
- Harvey, M. C., P. J. White, K. M. MacKenzie, and B. G. Lovelock (2011), Results from a soil CO<sub>2</sub> flux and shallow temperature survey at the San Jacinto-Tizate geothermal power project, Nicaragua, *New Zealand Geothermal Workshop Proceedings*.
- Harvey, M. C., Rowland, J. V., Chiodini, G., Rissmann, C. F., Bloomberg, S., Hernández, P. A., Mazot, A., Viveiros, F., and Werner, C. (2015a). Heat flux from magmatic hydrothermal systems related to availability of fluid recharge. *Journal of Volcanology and Geothermal Research*, 302, 225-236.
- Harvey, M. C., Zygadlo, M., and Dwivedi, A. (2015b), Use of isotopic analysis to distinguish between biological and geothermal soil CO<sub>2</sub> flux at Tauhara and Te Mihi geothermal areas. In *Proceedings 37<sup>rd</sup> New Zealand Geothermal Workshop*.
- Harvey Geoscience (2017), Soil CO<sub>2</sub> Flux and Shallow Temperature Survey San Jacinto, March-April 2017. Client Report.
- Norini (2016), Volcanotectonic study of the San Jacinto-Tizate concession and implications for the geothermal exploration. Client report.
- Olaya, V., & Conrad, O. (2009). Geomorphometry in SAGA. *Developments in Soil Science*, 33, 293-308.
- Raich, J. W., and Schlesinger, W. H. (1992). The global carbon dioxide flux in soil respiration and its relationship to vegetation and climate. *Tellus B*, 44, 81-99.
- Ratouis, T. M., & Zarrouk, S. J. (2016), Factors controlling large-scale hydrodynamic convection in the Taupo Volcanic Zone (TVZ), New Zealand. *Geothermics*, 59, 236-251.
- Reimann, C., Filzmoser, P., & Garrett, R.G. (2005), Background and threshold: critical comparison of methods of determination. *Science of the Total Environment*, Vol. 346, pp. 1-16.
- Remy, N., Boucher, A., & Wu, J. (2009), *Applied geostatistics with SGeMS: A user's guide*. Cambridge University Press.
- Rissmann, C., B. Christenson, C. Werner, M. Leybourne, J. Cole, and D. Gravley (2012), Surface heat flow and CO<sub>2</sub> emissions within the Ohaaki hydrothermal field, Taupo Volcanic Zone, New Zealand, *Appl. Geochem.*, 27, 223-239.
- SKM (2011), San Jacinto - Interpretation of 2011 Gravity and magnetic surveys. Client report.
- SKM (2012), Well SJ11-1 Geology and Petrology Report. Client Report.
- Werner, C., Hochstein, M. P., & Bromley, C. (2004). CO<sub>2</sub> fluxes of steaming ground at Karapiti (Wairakei, NZ). In *The 26th New Zealand Geothermal Workshop/GEO3, Taupo, New Zealand*.